LETTERS

Generation of electron beams carrying orbital angular momentum

Masaya Uchida[1] & Akira Tonomura[1]

All forms of waves can contain phase singularities[1–4]. In the case of optical waves, a light beam with a phase singularity carries orbital angular momentum, and such beams have found a range of applications in optical manipulation, quantum information and astronomy[3–9]. Here we report the generation of an electron beam with a phase singularity propagating in free space, which we achieve by passing a plane electron wave through a spiral phase plate constructed naturally from a stack of graphite thin films. The interference pattern between the final beam and a plane electron wave in a transmission electron microscope shows the 'Y'-like defect pattern characteristic of a beam carrying a phase singularity with a topological charge equal to one. This fundamentally new electron degree of freedom could find application in a number of research areas, as is the case for polarized electron beams.

Angular momentum is one of the most fundamental physical quantities, both in classical and quantum mechanics. Light beams can carry not only spin angular momentum, which is associated with their polarization state, but also orbital angular momentum (OAM)[3–5]. The OAM contribution is directly linked to the topology of wavefronts and phase singularities. When the wavefronts have a spiral shape, there is a phase singularity (Fig. 1). Light beams with non-zero topological charge (l) carry an OAM quantized in units of $l\hbar$ per photon, where $\hbar$ is Planck's constant h divided by 2π (refs 3–5). At its centre, the beam has a spiral-type phase singularity (also known as an optical vortex, a topological defect, or a wave dislocation), where the intensity is zero and the phase is undetermined. The order of the phase singularity is evaluated as the circulation of the phase gradient about the singularity[1], $\oint_C \nabla\phi \cdot \mathrm{d}\mathbf{s} = 2\pi l$. Here, ϕ is the phase and $\mathbf{s}$ is the unit vector tangential to the closed path C around which the loop integral is taken.

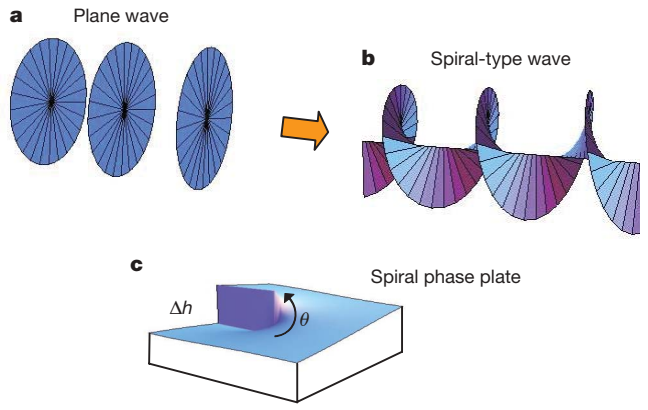

Figure 1 | Conversion from a plane wave to a spiral-type wave using a spiral phase plate. a, Wavefronts of a plane wave, which are planes normal to the propagation axis. **b**, Wavefronts of a spiral-type wave. When the wavefronts have a spiral shape so that a $2l\pi$ variation of the phase occurs in a 2π rotation around the beam axis, where l is a topological charge that denotes the winding number of the spiral, there is a phase singularity at the centre. The sign of l represents right-handed or left-handed ramps. **c**, Spiral phase plate with a step height Δh. The thickness increases continuously in proportion to the azimuthal angle θ, but is constant in the radial direction. When a plane wave passes through the spiral phase plate, a spiral wavefront character is imprinted on the plane wave, where a phase singularity at the core of the beam is generated. By changing the step height or material, spiral beams with various l values can be produced.

Phase singularities in waves can be observed in nature. The concept of wave phase singularities was first established in ref. 1. The study of phase singularities, both quantized and classical, is now a rich and diverse topic of fundamental and applied research [2–4]. In this context, it is of great interest to investigate electron beams with phase singularities (or OAM); to our knowledge, no experimental measurements of such electron beams have been reported. However, there have been related theoretical studies, such as the detection of magnetic monopoles by electron holography[10,11] and the phase retrieval method in the presence of phase singularities[12]. Recently, it has been shown[13] that electron wave packets can carry a well-defined OAM, using the semi-classical paraxial solutions of the Schrödinger equation with phase singularities. The present experiment confirms the prediction[13] of quantum electron waves carrying OAM.

Phase singularities in light beams can be artificially created by several methods[3,4], using cylindrical lenses[14], spiral phase plates[15–17] and synthesized holograms[18–20]. They can also be formed by light scattering from rough surfaces[2], and even by regular light wave interference[21]. In the present study, we generated an electron beam containing a phase singularity by using a spiral-like phase plate. Phase plates modify the wavefront structure of the incident wave. The phase shift of photons or electrons can be controlled by varying the thickness of the material (see Methods). Typically, the thickness of a spiral phase plate increases in proportion to the azimuthal angle θ around a point in the centre of the plate (Fig. 1c). When a plane wave passes through such a spiral phase plate, a spiral wavefront character is imprinted on the incident plane wave, where a phase singularity at the core of the beam is generated. A common method to visualize phase singularities is based on interference with a plane wave[3,4]. The signature of phase singularities corresponds to the appearance of a 'fork', or 'Y'-shape, in the interference fringe.

Spiral phase plates for light beams have been fabricated by conventional machining[16] and optical[15] or electron[17] lithography. But for electrons, it is not easy to fabricate a spiral phase plate with continuously changing thickness, because of its small size. For example, to obtain a spiral phase plate that is able to generate electron beams with a topological charge $l = \pm 1$ (2π phase change), the step height of the spiral phase plate is about 84 nm, for Si and using a 300 kV electron beam. Therefore, it was our aim to find a simpler spiral phase plate. One promising way is to make spiral-like linear phase plates[22]. A spiral-like

[1]Advanced Science Institute, RIKEN (The Institute of Physical and Chemical Research), Wako, Saitama 351-0198, Japan.

linear plate is divided into several regions with constant thickness. Simulated interference patterns for the spiral (Fig. 2a) and spiral-like linear (Fig. 2b) phase plates producing a beam with a topological charge $l = 1$ are shown in Fig. 2c and d, respectively. When a wave with $l = 1$ interferes with a plane wave, a 'Y'-like defect pattern in the interference pattern shows up, which is analogous to edge dislocations appearing in atomic crystals or those in helimagnets[23]. For higher orders $|l| \geq 2$, a splitting of the interference fringe into three or more new fringes appears[18]. For a spiral-like linear phase plate, an additional radial discontinuity in the interference fringes occurs.

Here we used spontaneously stacked graphite thin films as a spiral-like phase plate. They were prepared by crushing a pencil lead into fine fragments, which were then dispersed on Cu grids coated with a carbon support film. Figure 3a shows an overfocused transmission electron microscope (TEM) image of a graphite thin film, where the image contrast or intensity is roughly proportional to the sample thickness (see Methods). The typical graphite film thickness is 10–100 nm, which is suitable for the required phase change. It was frequently observed that several graphite thin films were stacked spontaneously. We note that a spiral-like structure can be seen within the red box in Fig. 3a. The spiral-like structure of the phase plate extends around 10 nm from the centre (Fig. 3b). By passing a plane electron wave through this region, electron beams with phase singularities could be generated.

To characterize the phase structure of the electron beam leaving the phase plate, we used the electron interference method[24]. The interference experiments were done in a TEM (Hitachi HF-3000X) equipped with a field emission gun and an electron biprism (Fig. 3c). The accelerating voltage of the electron beam used here was 300 kV and the corresponding wavelength is 1.97 pm. The electron beam is split into two by a biprism: one of the beams passes through the phase plate; the other is a reference plane electron wave. Both beams were directed to a screen to form a hologram. A hologram shows a 'Y'-like defect pattern (Fig. 3d), which is the characteristic signature of a screw-type phase singularity with topological charge $l = 1$. Figures 3e and f show respectively a phase distribution obtained from the hologram in Fig. 3d using the software HoloWorks[25] and a computer-reconstructed interference image. The phase change around the centre occurs on a nanometre scale. The computer-reconstructed interference pattern in Fig. 3f shows a clear 'Y'-like defect pattern. The phase step as seen in Fig. 3g is near 2π, which results in non-integer l values[26]. Such a non-2π phase step is reflected as a radial abrupt phase shift along the step of the phase plate in Fig. 3f. The phase jump can be estimated as occurring over an azimuthal range of less than 2.5°.

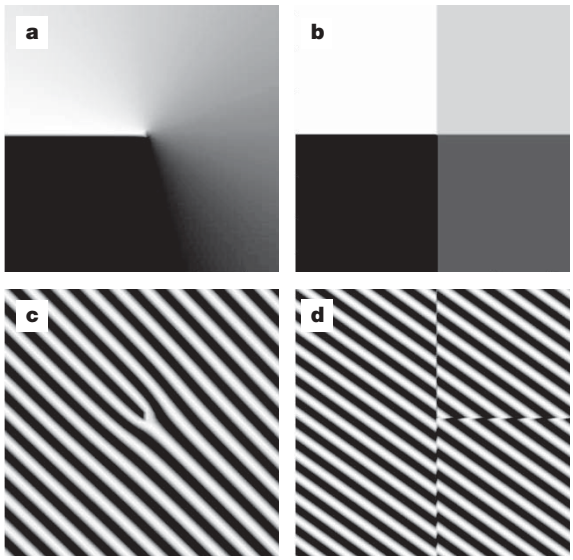

Figure 2 | Phase distributions and simulated interference patterns for the spiral and spiral-like linear phase plates. **a**, Phase distribution of a spiral phase plate, with the phase step 2π producing a beam with a topological charge $l = 1$, presented as a grey-scale image, where black and white represent 0 and 2π, respectively. The phase changes continuously from 0 to 2π around the centre. **b**, Phase distribution of a spiral-like linear phase plate producing a beam with $l = 1$. The phase changes as a spiral staircase from 0 to 2π around the centre. **c**, **d**, Simulated interference patterns between a plane wave and a beam passing through the phase plate in **a** (**c**) or **b** (**d**). The signature of the presence of a phase singularity is a 'Y'-like defect in the fringe pattern, where a new fringe starts at the location of the phase singularity. An additional discontinuity in the interference fringes in **d** occurs. For negative l, this 'Y' is directed down.

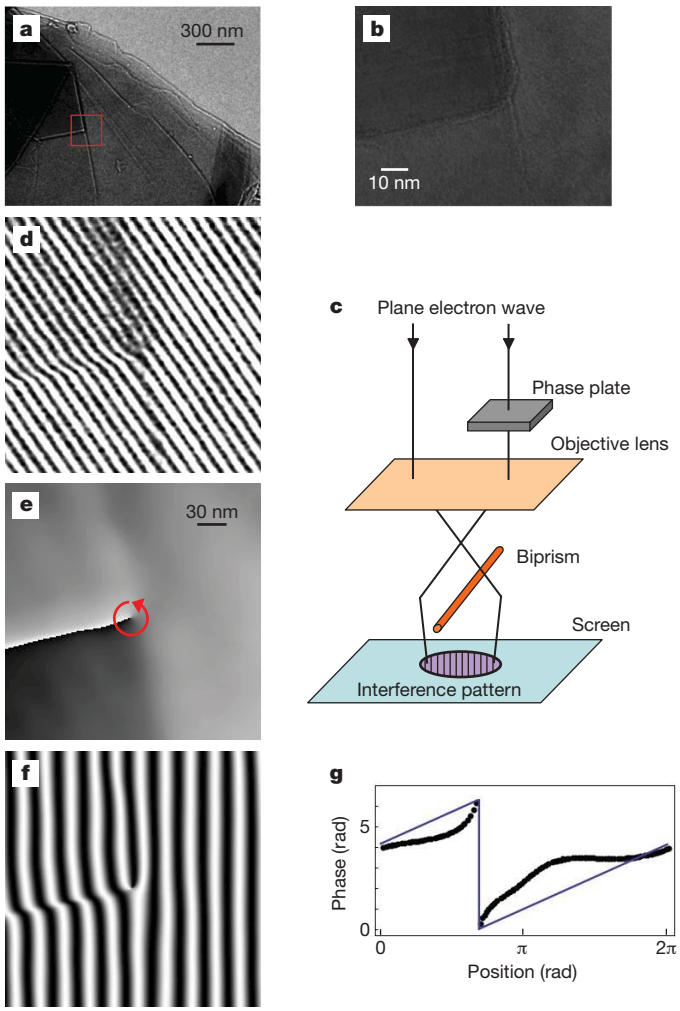

Figure 3 | Spiral-like phase plate composed of graphite thin films and the phase singularity in the electron interference pattern. **a**, Overfocused TEM image of spontaneously stacked graphite thin films. The spiral-like structure can be seen within the red box. **b**, High-magnification TEM image of the spontaneously stacked graphite thin films near the centre region, obtained by a JEM-3010 TEM operated at 200 kV. The spiral-like structure of the phase plate extends around 10 nm from the centre. Note that the phase singularity (orbital angular momentum, OAM) of the electron beams is created not by the core structure of the spiral phase plate, but by the wavefront structure. **c**, Schematic diagram for electron hologram formation. A field emission gun provides coherent electron illumination. The spiral-like phase plate modifies a wavefront of a plane electron wave and the biprism enables overlap of the beams passing through the phase plate and the plane electron wave. **d**, The experimentally obtained interference pattern (hologram) corresponding to the region shown in the red box in **a**. In the centre of the hologram, a 'Y'-like defect pattern is observed, which is the signature of the phase singularity with $l = 1$. The potential field applied to the biprism filament is 85 V and the interference fringe spacing is about 12 nm. **e**, Phase distribution reconstructed from the hologram in **c**. White and black regions correspond to a phase of 2π and 0, respectively. **f**, A computer-reconstructed interference image from the phase image in **e**. The radial abrupt phase shift is due to the non-2π phase step and the non-abrupt phase jump. **g**, A phase profile obtained along the circle indicated in **e** (black dots). The phase step is near 2π within an azimuthal range of 2.5°. The blue line represents a phase profile for an ideal spiral phase plate.

We have observed similar 'Y'-like defect patterns for other sample regions, which suggests that the generation of electron beams with phase singularities is a common phenomenon when electrons are scattered by materials with thickness that is inhomogeneous on the nanoscale. For the reproducible production of electron beams with topological charge, better spiral phase plates will be needed—methods such as the focused ion beam technique might be suitable to produce them. Although we cannot find experimental evidence for electron beams with topological charge of higher orders, $|l| \geq 2$, we would expect such electron beams could be produced by increasing or designing the step height of the phase plate. The 'Y'-like defect pattern observed in the interference patterns indicates the possible existence of OAM states in the electron beam. We note that OAM of photon beams has been directly confirmed through measurements of the rotation of a beam by a cylindrical lens[3,5] and by particles[3,6], and by the interferometric method[3]. Any interaction between electron beams with OAM and matter might be accompanied by an exchange of momentum. Future research should measure the OAM of electron beams directly.

Another striking feature of optical phase singularities is that they appear as zero intensity, in a ring-like intensity profile in the beam cross-section, owing to complete destructive interference[3,15,16]. However, we could not detect any dark core in the Fourier plane. This is because of the small size of the dark core due to the short electron wavelength. The radius of the first ring in the Fourier plane of the beam with $l = 1$ is approximated by $\rho \approx 2.4\lambda f/(2\pi R)$ (ref. 17), where λ is the electron wavelength, f is the focal length and R is the radius of a plane wave beam formed by a circular aperture. In our case ($\lambda = 1.97$ p.m., $f = 3$ mm, $R = 1$ μm), the radius would be about 2.3 nm.

In summary, we have generated electron beams with a phase singularity and OAM by passing a plane wave through a spiral-like phase plate composed of graphite thin films. The signature of the phase singularity with $l = 1$ has been revealed by electron holography as a 'Y'-like defect pattern in the interference patterns. A simple application of such electron beams would be contrast enhancement in electron microscopy. It has been shown that light beams with screw-type wavefronts are extremely sensitive to phase jumps or edges[27]. This application has some parallels with the phase contrast imaging method using a phase plate[28]; additional relative phase shift between scattered and unscattered electron waves is given by the mean inner potential of matter or the electrostatic potential of the lens electrode. Another idea in electron microscopy might be to take advantage of the transfer of OAM, leading to a new type of electron energy-loss spectroscopy (EELS). In the case of spin-polarized EELS, spin-polarized electrons are required, whereas the present method using a spiral phase plate can easily be implemented with existing standard electron microscopes, inserting the spiral phase plate into the beam pass. In this context, it should be also noted that energy loss chiral dichroism in a TEM allows information to be obtained about spin and orbital magnetic moments in the absence of spin-polarized electron beams[29]. Just as in the case of spin angular momentum associated with polarized electron beams, electron phase singularity with OAM is a new fundamental quantity. Use of electron beams carrying OAM is expected to lead to novel fields of research in several areas: examples include condensed-matter spectroscopy, new electron microscopes, and particle physics.

METHODS SUMMARY

Electron phase shift. Electron phase shift (sample thickness) can be measured by electron holography[24]. In the absence of dynamical diffraction effects, and ignoring any magnetic and other electrostatic potentials associated with the sample, the phase shift $\phi(x, y)$ of the electron wave passing through the sample (thickness t) can be written

$$\phi(x, y) = C_E V(x, y) t(x, y)$$

where C_E is a sample-independent constant ($C_E = 0.00652\ \mathrm{rad\ V^{-1}\ nm^{-1}}$ when the acceleration voltage is 300 kV), $V(x, y)$ is the mean inner potential of the sample, and x and y are directions perpendicular to the electron beam. For graphite in our case the mean inner potential $V(x, y)$ is 11–13 V (ref. 30). Then, the sample thickness is 88–74 nm, giving the phase shift 2π. For Si $V(x, y)$ is 11.5 V, giving a sample thickness of 84 nm.

Received 18 August 2009; accepted 12 February 2010.

1. Nye, J. F. & Berry, M. V. Dislocations in wave trains. *Proc. R. Soc. Lond. A* **336,** 165–190 (1974).
2. Nye, J. F. *Natural Focusing and Fine Structure of Light* (Institute of Physics Publishing, 1999).
3. Allen, L., Barnett, S. M. & Padgett, M. J. (eds) *Optical Angular Momentum* (Taylor & Francis, 2003).
4. Padgett, M., Courtial, J. & Allen, L. Light's orbital angular momentum. *Phys. Today* **57** (5), 35–40 (2004).
5. Allen, L., Beijersbergen, M. W., Spreeuw, R. J. C. & Woerdman, J. P. Orbital angular momentum of light and the transformation of Laguerre-Gaussian modes. *Phys. Rev. A* **45,** 8185–8190 (1992).
6. He, H., Friese, M. E. J., Heckenberg, N. R. & Rubinsztein-Dunlop, H. Direct observation of transfer of angular momentum to absorptive particles from a laser beam with a phase singularity. *Phys. Rev. Lett.* **75,** 826–829 (1995).
7. Paterson, M. *et al.* Controlled rotation of optically trapped microscopic particles. *Science* **292,** 912–914 (2001).
8. Mair, A., Vaziri, A., Weihs, G. & Zeilinger, A. Entanglement of the orbital angular momentum states of photons. *Nature* **412,** 313–316 (2001).
9. Molina-Terriza, G., Torres, J. P. & Torner, L. Twisted photons. *Nature Phys.* **3,** 305–310 (2007).
10. Fukuhara, A., Shinagawa, K., Tonomura, A. & Fujiwara, H. Electron holography and magnetic specimens. *Phys. Rev. B* **27,** 1839–1843 (1983).
11. Tonomura, A. Applications of electron holography. *Rev. Mod. Phys.* **59,** 639–669 (1987).
12. Allen, L. J., Faulkner, H. M. L., Oxley, M. P. & Paganin, D. Phase retrieval and aberration correction in the presence of vortices in high-resolution transmission electron microscopy. *Ultramicroscopy* **88,** 85–97 (2001).
13. Bliokh, K. Y., Bliokh, Y. P., Savel'ev, S. & Nori, F. Semiclassical dynamics of electron wave packet states with phase vortices. *Phys. Rev. Lett.* **99,** 190404 (2007).
14. Beijersbergen, M. W., Allen, L., van der Veen, H. E. L. O. & Woerdman, J. P. Astigmatic laser mode converters and transfer of orbital momentum. *Opt. Commun.* **96,** 123–132 (1993).
15. Khonina, S. N., Kotlyar, V. V., Shinkaryev, M. V., Soifer, V. A. & Uspleniev, G. V. The phase rotor filter. *J. Mod. Opt.* **39,** 1147–1154 (1992).
16. Beijersbergen, M. W., Coerwinkel, R. P. C., Kristensen, M. & Woerdman, J. P. Helical-wavefront laser beams produced with a spiral phaseplate. *Opt. Commun.* **112,** 321–327 (1994).
17. Kotlyar, V. V. *et al.* Diffraction of a plane, finite-radius wave by a spiral phase plate. *Opt. Lett.* **31,** 1597–1599 (2006).
18. Bazhenov, V., Yu., Vasnetsov, M. V. & Soskin, M. S. Laser beams with screw dislocations in their wavefronts. *Sov. JETP Lett.* **52,** 429–431 (1990).
19. Heckenberg, H. R., McDuff, R., Smith, C. P. & White, A. G. Generation of optical phase singularities by computer-generated holograms. *Opt. Lett.* **17,** 221–223 (1992).
20. Basistiy, I., Bazhenov, V., Yu., Soskin, M. S. & Vasnetsov, M. V. Optics of light beams with screw dislocations. *Opt. Commun.* **103,** 422–428 (1993).
21. Angelsky, O. V., Besaha, R. N. & Mokhun, I. I. Appearance of wave front dislocations under interference among beams with simple wave fronts. *Opt. Appl.* **27,** 273–278 (1997).
22. Kim, G. H. *et al.* Optical vortices produced with a nonspiral phase plate. *Appl. Opt.* **36,** 8614–8621 (1997).
23. Uchida, M., Onose, Y., Matsui, Y. & Tokura, Y. Real-space observation of helical spin order. *Science* **311,** 359–361 (2006).
24. Tonomura, A. *Electron Holography* (Springer, 1999).
25. Völkl, E., Allard, L. F. & Frost, B. J. A software package for the processing and reconstruction of electron holograms. *Microscopy* **180,** 39–50 (1995).
26. Leach, J., Yao, E. & Padgett, M. J. Observation of the vortex structure of a non-integer vortex beam. *N. J. Phys.* **6,** 71 (2004).
27. Fürhapter, S., Jesacher, A., Bernet, S. & Ritsch-Marte, M. Spiral phase contrast imaging in microscopy. *Opt. Express* **13,** 689–694 (2005).
28. Majorovits, E. *et al.* Optimizing phase contrast in transmission electron microscopy with an electrostatic (Boersch) phase plate. *Ultramicroscopy* **107,** 213–226 (2007).
29. Schattschneider, P. Exchange of angular momentum in EMCD experiments. *Ultramicroscopy* **109,** 91–95 (2008).
30. Sánchez, A. & Ochando, M. A. Calculation of the mean inner potential. *J. Phys. C* **18,** 33–41 (1985).

Acknowledgements Discussions with F. Nori, H. Ichinose and K. Sawada of RIKEN are acknowledged.

Author Contributions M.U. had the idea of doing this experiment, fabricated the phase plate, performed the TEM experiments, analysed and interpreted the data, simulated the interference patterns, and wrote the manuscript; A.T. coordinated the work on the TEM.

Author Information Reprints and permissions information is available at www.nature.com/reprints. The authors declare no competing financial interests. Correspondence and requests for materials should be addressed to M.U. (masaya1.uchida@gmail.com).